



**HAL**  
open science

## Evidence for face selectivity in early vision

Florence Campana, Jacob Martin, Levan Bokeria, Simon Thorpe, Xiong Jiang, Maximilian Riesenhuber

► **To cite this version:**

Florence Campana, Jacob Martin, Levan Bokeria, Simon Thorpe, Xiong Jiang, et al.. Evidence for face selectivity in early vision. 2020. hal-03032067

**HAL Id: hal-03032067**

**<https://hal.science/hal-03032067>**

Preprint submitted on 30 Nov 2020

**HAL** is a multi-disciplinary open access archive for the deposit and dissemination of scientific research documents, whether they are published or not. The documents may come from teaching and research institutions in France or abroad, or from public or private research centers.

L'archive ouverte pluridisciplinaire **HAL**, est destinée au dépôt et à la diffusion de documents scientifiques de niveau recherche, publiés ou non, émanant des établissements d'enseignement et de recherche français ou étrangers, des laboratoires publics ou privés.

1 **Title: Evidence for face selectivity in early vision**

2 **Classification: Biological Sciences (Psychological and Cognitive Sciences)**

3

4 **Authors:** Florence Campana<sup>1</sup>, Jacob G. Martin<sup>1,2</sup>, Levan Bokeria<sup>1</sup>, Simon Thorpe<sup>2</sup>, Xiong Jiang<sup>1</sup>,  
5 Maximilian Riesenhuber<sup>1\*</sup>.

6 **Affiliations:**

7 <sup>1</sup>Department of Neuroscience, Georgetown University Medical Center, Research Building, Room  
8 WP-12, 3970 Reservoir Rd. NW, Washington, District of Columbia 20007, USA

9 <sup>2</sup>Centre de Recherche Cerveau & Cognition, CNRS-Université Toulouse 3, 31059 Toulouse,  
10 France

11

12 \*Corresponding authors: [mr287@georgetown.edu](mailto:mr287@georgetown.edu) ; [campana.florence@gmail.com](mailto:campana.florence@gmail.com)

13

14 Number of pages : 52

15 Number of figures : 4

16 Number of words : Abstract (128), Significance Statement (119), Introduction (545), Discussion  
17 (1415).

18

19 Conflict of Interest: The authors declare no competing financial interests.

20

21  
22  
23  
24  
25  
26  
27  
28  
29  
30  
31  
32  
33  
34  
35  
36  
37  
38  
39  
40

Acknowledgments: This research was supported by National Eye Institute Grant R01EY024161 and a grant from the Agence Nationale de la Recherche ANR-13-NEUC-004-01. We thank Dr. Alex Todorov for face stimuli, and Drs. Bobby Stojanoski and Rhodri Cusack for scrambling code, and Rebekah Farris for help with experiments.

## 41 **Abstract**

42 The commonly accepted “simple-to-complex” model of visual processing in the brain posits that  
43 visual tasks on complex objects such as faces are based on representations in high-level visual  
44 areas. Yet, recent experimental data showing the visual system’s ability to localize faces in natural  
45 images within 100ms (Crouzet et al., 2010) challenge the prevalent hierarchical description of the  
46 visual system, and instead suggest the hypothesis of face-selectivity in early visual areas. In the  
47 present study, we tested this hypothesis with human participants in two eye tracking experiments,  
48 an fMRI experiment and an EEG experiment. We found converging evidence for neural  
49 representations selective for upright faces in V1/V2, with latencies starting around 40 ms post-  
50 stimulus onset. Our findings suggest a revision of the standard “simple-to-complex” model of  
51 hierarchical visual processing.

## 52 **Significance statement**

53 Visual processing in the brain is classically described as a series of stages with increasingly  
54 complex object representations: early visual areas encode simple visual features (such as oriented  
55 bars), and high-level visual areas encode representations for complex objects (such as faces). In  
56 the present study, we provide behavioral, fMRI, and EEG evidence for representations of complex  
57 objects – namely faces – in early visual areas. Our results challenge the standard “simple-to-  
58 complex” model of visual processing, suggesting that it needs to be revised to include neural  
59 representations for faces at the lowest levels of the visual hierarchy. Such early object  
60 representations would permit the rapid and precise localization of complex objects, as has  
61 previously been reported for the object class of faces.

62

63

## 64 Introduction

65 According to the standard model of visual processing (Hubel & Wiesel, 1962 ; Maunsell &  
66 Newsome, 1987 ; Riesenhuber & Poggio, 2002), simple physical features (e.g., luminance and  
67 edges) are encoded first, in low-level visual areas such as V1, while more complex shape features  
68 are encoded later in intermediate visual areas such as V4. Complex object categories (e.g., faces  
69 and objects) are thought to be encoded in high-level visual areas such as the Fusiform Face Area  
70 (FFA).

71 Humans are able to report the presence of specific objects (e.g. an animal or a vehicle) in natural  
72 cluttered scenes as early as 250 ms post-stimulus onset ((Fabre-Thorpe et al., 2003; Poncet et al.,  
73 2012; Thorpe et al., 1996; VanRullen and Thorpe, 2001). Those latencies are short, but compatible  
74 with a progression of the neural activity from low-level to high-level visual areas, then followed  
75 by the formation of a decision-variable in the frontal cortex (Freedman et al., 2003; Riesenhuber  
76 & Poggio, 2000). However, the recent use of saccadic response paradigms, rather than manual  
77 response paradigms, has revealed that object detection can be achieved substantially faster than  
78 previously thought. Faces, for instance, can be saccaded to within 100 ms following stimulus onset  
79 (Crouzet et al., 2010). Since conduction delays to generate an oculomotor response take around  
80 20-35 ms (Heeman et al., 2017), this suggests that the visual detection has already been made by  
81 65-80 ms following stimulus onset. Such latencies pose a challenge for the standard hierarchical  
82 view of the visual system. A second remarkable feature of these ultra-rapid saccades is their  
83 localization accuracy: subjects are able to trigger saccades accurately toward very small faces of  
84 1° visual angle pasted at an eccentricity of 7° in a complex cluttered scene, after only 120 ms  
85 (Brilhault et al., 2011). V1/V2 neurons are a possible candidate since their receptive fields subtend

86 1° in humans at 7° eccentricity (Dumoulin & Wandell, 2008), with the earliest responses starting  
87 45 ms post-stimulus onset (Foxy et al., 2008). By contrast, V4 receptive fields may be too large  
88 since they subtend 4°-6° at 6° eccentricity in humans (Motter 2009).

89 The precision of those saccades in cluttered environments and the fact that they start as early as  
90 “express saccades” – the fastest known saccades in humans, that are directed toward luminous dots  
91 (Fischer et al., 1984) – suggest that early visual areas, which are characterized by small receptive  
92 fields and short activation latencies, might contain representations of complex object categories  
93 such as faces.

94 In the present study, we tested the hypothesis of face-selective representation in early visual areas  
95 using a multi-pronged approach. Specifically, to probe the temporal characteristics of putative  
96 early face-specific responses, we conducted two eye-tracking experiments and an EEG  
97 experiment. To probe the spatial characteristics of putative early face-specific responses, we  
98 conducted a functional Magnetic Resonance Imaging (fMRI) experiment. In order to link the  
99 results across experiments, stimuli were similar across experimental techniques. They consisted in  
100 small faces of 2° size, to match the size of V1/V2 receptive fields. We here report converging  
101 evidence that faces elicit specific responses in V1/V2 as early as 40 ms post-stimulus onset. This  
102 finding suggests a more nuanced picture of visual hierarchical processing than the traditional  
103 “simple-to-complex” model, namely one in which early areas contains neuronal representations  
104 selective for complex objects.

105

## 106 **Material and Methods**

107 Across all studies, all subjects were naïve as to the purpose of the study, gave their written  
108 informed consent before participating, and were paid for their participation. The Institutional  
109 Review Board of Georgetown University approved the study.

### 110 Experiment 1: Specificity of ultra-rapid face detection

#### 111 Experimental Design

112 **Participants.** Eight (6 women,  $22.3 \pm 1.9$  years old across all subjects) healthy, right-handed  
113 human subjects with normal or corrected-to-normal vision took part in the experiment.

114

115 **Stimuli.** The stimuli used in the experiment were natural scenes ( $n=15$ , resolution  $15^\circ \times 20^\circ$  of  
116 visual angle, from an online database) in which items (faces and distractors) were pasted. To avoid  
117 that pasted items pop-out, the contrast histogram of the pasted item was stretched so that that the  
118 bottom 1% and top 1% from the pixels of this item match the bottom 1% and top 1% from the  
119 pixel values of the patch of natural scene replaced. All the images were grayscale.

120 Items were pasted at one of four locations at  $7^\circ$  visual eccentricity from the center of the screen:

121  $25^\circ$  or  $45^\circ$  above and below the horizontal meridian, on the left and right side of the screen. This

122 asymmetrical spatial configuration aimed at activating the primary visual cortex at symmetrical

123 sites on the lower and upper banks of the calcarine fissure (Di Russo et al., 2005) granted that the

124 horizontal meridian is represented in the lower bank of the calcarine fissure (Aine et al., 1996). To

125 approximately match the size of the receptive fields in V1/V2 at  $7^\circ$  eccentricity (Dumoulin &

126 Wandell, 2008), all faces and distractors were resized to span  $2^\circ$  of visual angle (along the height

127 dimension).  $7^\circ$  eccentricity was chosen to be in the range of the eccentricity used in (Brilhault et

128 al., 2011), in which fast saccades toward faces were observed. 15 emotionally neutral faces of  
129 males generated with the FaceGen 3.1 software development kit (Singular Inversions, Toronto,  
130 Canada) were used. Elements external to the faces (necks and shoulders) were manually removed.  
131 From those faces, new face images (inverted, configuration-scrambled and phase-scrambled faces)  
132 were created using the Gimp image manipulation program (<https://www.gimp.org/>) and MATLAB  
133 (The Mathworks, MA): “configuration-scrambled” faces in which the internal features (the eyes,  
134 the nose and mouth) were positioned at random places, inverted faces, and phase-scrambled face  
135 (Xu et al., 2005). 15 images of houses (online database) were also used as distractors (Figure 1A).  
136 In this experiment, the “configuration-scrambled” faces, the inverted faces, the phase-scrambled  
137 faces and the houses are called "distractors".

138

139 **Procedure.** Stimuli were presented on a computer screen at a viewing distance of 60 cm (refresh  
140 rate 60Hz, resolution 1024\*768, 24\*18° visual angle). Eye movements were recorded using a  
141 camera-based eye tracker (SR research, Eyelink 1000 Plus) with a temporal resolution of 2000 Hz.  
142 A chin and headrest helped the subjects to stabilize their head. Each trial started with a white  
143 fixation cross. Subjects had to keep their eyes on the cross (within a box of radius 1° of visual  
144 angle) for 150 ms for the natural scene to be displayed. A 200-ms gray screen was displayed  
145 between the end of the fixation and the start of the natural image. This gap enables a faster initiation  
146 of saccades (Fischer & Weber, 1993, Kirchner & Thorpe, 2006, Crouzet et al., 2010). Subjects  
147 were instructed to saccade as quickly as possible toward the face pasted in the natural scene. The  
148 natural scene was displayed until the subject’s eyes gazed at the face for 150 consecutive ms in a  
149 square zone centered on the face and of 2° width. Next fixation started after a pseudo-random  
150 interval (1000-1200 ms). Subjects performed 15 blocks of 72 trials each. Within a block, there

151 were 48 trials with a face and a distractor (12 possible spatial configurations, one per distractor  
152 category), 12 trials with a face only (4 positions, each repeated 3 times), and 12 trials with two  
153 faces presented simultaneously (6 possible spatial configurations, each repeated twice). To assess  
154 the effect of the different distractor categories independently of face identity, the identity of the  
155 face and of the distractor (inverted, scramble or configuration-scrambled) were always the same  
156 within an image. Each of the 15 backgrounds and each of the 15 face identities were displayed 72  
157 times (pseudo-random association of a face with a background).

158 Subjects were informed that, in any trial, the faces would appear at 1 out of 4 possible locations  
159 (left up, left bottom, right up, right bottom) (Figure 1A). They were informed that the images  
160 would contain distractors, some of them sharing similarities with faces, but that only the “normal  
161 faces” were relevant for the task.

162

### 163 Statistical Analyses

164 The position of the left eye from each participant was recorded during the whole experiment,  
165 every half ms. Only the first saccade within each trial was kept in the analysis. For each  
166 distractor condition, we computed the percentage of saccades landing in the quadrant with a face,  
167 in the quadrant with a distractor, and in empty quadrants. This measure was averaged across  
168 subjects. We also computed saccadic reaction times, measured as the duration elapsed between  
169 the display of the stimulus and the initiation of the saccade, as recorded by the eye tracker. This  
170 measure was averaged across subjects too. We computed the minimum saccadic reaction times  
171 (SRT), which is a statistical estimate of the latency at which correct saccades start to be more  
172 numerous than saccades toward the distractor’s quadrant (Crouzet et al., 2010). For each subject,  
173 we computed the cumulative count of number of saccades whose SRT was inferior to a cutoff

174 value, step size 1 ms. We then searched for at least 20 consecutive bins with significantly more  
175 correct than erroneous responses using a chi-square test with a criterion of  $p < 0.05$ . The first of  
176 those bins was considered to correspond to the minimum SRT.

## 177 Experiment 2: Timing and spatial accuracy of ultra-rapid face detection

### 178 Experimental design

179 **Participants.** Sixteen (14 women,  $23.6 \pm 4.1$  years old across all subjects) healthy, right-handed  
180 human subjects with normal or corrected-to-normal vision took part in the experiment.

181 **Stimuli.** Stimuli consisted of annuli (radius:  $7^\circ$  of visual angle, width:  $2.5^\circ$  of visual angle) cut out  
182 from the same database of natural scenes as used in Experiment 1. In each trial, a face (height:  $2^\circ$   
183 of visual angle) was pasted at a random polar angle, always at  $7^\circ$  eccentricity from the center of  
184 the screen (Figure 2A). 48 grayscale scenes with a high degree of clutter were selected after visual  
185 inspection to make sure that, after the procedure of luminance equalization described above, the  
186 pasted faces were still clearly visible at any position within at least 2 out of 4 quadrants in the  
187 annulus. 36 grayscale photographs of adult faces of various ethnicities were used (online database)  
188 to maximize the ecological value of our results. The neck and shoulders were manually removed  
189 from those images as in Experiment 1. Eye movements were recorded using the same setup as in  
190 Experiment 1.

191

192 **Procedure.** The experimental setup was identical to that of Experiment 1 except that the distance  
193 between the subjects' eyes and the screen was 93 cm (60 cm for the two first subjects, but stimulus  
194 size in degrees of visual angle was identical). 36 faces were displayed, and subjects were instructed  
195 to saccade as quickly as possible to the faces. Similarly to Experiment 1, once the participant's  
196 gaze was within the face for 150 consecutive ms, the next trial started after a pseudo-random

197 interval (between 1000 and 1200 ms). Each face was displayed once within each quadrant (36 \* 4  
198 = 144 trials).

199

## 200 Statistical Analyses

201 To assess the properties of the earliest saccades that can be selectively oriented toward faces, only  
202 the first saccade of each trial was kept for analysis. We computed the minimum saccadic reaction  
203 times (SRT) with the same method as described in Experiment 1.

204

## 205 Experiment 3: EEG

### 206 Experimental Design

207 **Participants.** 21 healthy (9 women,  $24 \pm 4.2$  years old across old subjects), right-handed human  
208 subjects with normal or corrected-to-normal vision took part in the experiment. 2 subjects out of  
209 21 were removed from the group analysis (one since the image was removed in 30.6 % of the trials  
210 due to eye movements, the other due to the small amplitude of his N170 upright-face evoked  
211 component, at more than 3 std from the mean (average amplitude of the peak, left-presentation  
212 group, left-hemisphere:  $-4.3 \pm 1 \mu\text{V}$ , individual value for this participant:  $-0.49 \mu\text{V}$ ; on the right  
213 hemisphere:  $-4.7 \pm 1 \mu\text{V}$ , individual value:  $-1.7 \mu\text{V}$ ).

214 **Stimuli.** 100 different grayscale pictures of faces (the same as in the Experiment 2, plus 64 from  
215 the same database, from which the neck and shoulders were removed) were used in this  
216 experiment.

217

218 **Procedure.** The eyetracking setup was identical to that of Experiment 1. In 10 out of the 19 subjects  
219 included in the group analysis, eye movements were tracked with the Eyelink SR 1000 (for the

220 other subjects, eye movements could not be recorded because of difficulties with calibrating the  
221 eye tracker due to glasses and/or contact reflection). Scalp voltages were measured using an  
222 Electrical Geodesics (EGI, Eugene, OR) 128-channel Hydrocel geodesic sensor net and Net Amps  
223 300 amplifier. Incoming data were digitally low-pass filtered at 200 Hz and sampled at 500 Hz  
224 using common mode rejection with vertex reference. Impedances were set below 75 k $\Omega$  before  
225 recording began and maintained below this threshold throughout the recording session with regular  
226 impedance checks between blocks.

227

228 Half of the subjects ( $n = 9$ ) were presented with faces in the left visual field, among which 5 had  
229 their eye movements recorded. The other half was presented with faces in the right visual field ( $n$   
230  $= 10$ ), among which 5 had their eye movements recorded. Grayscale pictures of faces were  
231 displayed on a gray background on the horizontal meridian. We chose a gray background rather  
232 than a natural one to avoid a reduction of the amplitude of face-related signals (Cauchoix et al.,  
233 2014). To engage attention to the faces, as in Rossion & Caharel, 2011, we engaged subjects in a  
234 face categorization task (upright vs. inverted). The faces were either displayed at 1° eccentricity  
235 (height: 0.93° visual angle) or at 7° eccentricity (height: 2° visual angle), with eccentricity chosen  
236 randomly for each trial (50 faces at 1° eccentricity, 50 faces at 7° eccentricity). The faces size was  
237 determined using the cortical magnification factor in V1 whose value was computed from the  
238 formula in (Rousselet et al., 2005) so that, at the two presentation eccentricities, the faces stimulate  
239 similar portions of V1. Each trial began with a fixation point displayed for 300–600 ms followed  
240 by the brief display of a face, either upright or inverted, for 150 ms. 150ms was chosen as it is  
241 longer than our time window of interest (~50–100 ms) to avoid contamination of possible face-  
242 selective signals by stimulus-offset transient responses caused by the stimulus disappearance

243 (Macknik & Livingstone, 1998). Accurate stimulus timing was verified with a photodiode. The  
244 subjects then reported whether the face was upright or inverted by pressing the ‘1’ or ‘3’ key,  
245 respectively, with their right index and ring fingers (timeout: 2 seconds). After 600 ms, a new trial  
246 began. Subjects were asked to keep their eyes on the fixation point during the overall duration of  
247 a trial. Subjects were instructed to withhold eye blinks until the end of a trial and could pause the  
248 experiment between trials to blink and/or rest. For subjects whose eye movements were recorded,  
249 the face appeared only after 150 consecutive ms with the eyes on the fixation spot, thus extending  
250 the duration of the fixation in certain trials. For those subjects, the face was removed and the trial  
251 aborted if the subject was moving his/her eyes outside of the fixation point during the face  
252 presentation. The configuration (upright or inverted), the eccentricity and the identity of faces were  
253 pseudo-randomized and counterbalanced across the experiment. Subjects performed 10 blocks of  
254 100 trials each.

## 255 Statistical Analyses

256 **Data Analysis.** Data pre-processing and statistical analyses were performed using EEGLAB  
257 (Delorme & Makeig, 2004), FieldTrip (Oostenveld et al., 2011) and MATLAB (The Mathworks,  
258 MA). Noisy channels were interpolated. Data were band-pass filtered between 0.1 and 30 Hz with  
259 a causal filter. A causal filter was used in order to avoid shifts in the latency of the ERPs (Rousselet,  
260 2012). The filtered signal was then epoched from 150 ms before stimulus to 250 ms after the  
261 stimulus, baseline corrected in the [-150, 0] ms time window, and trials in which one of the facial  
262 channels was exhibiting a variation of more than 75  $\mu\text{V}$  in the [-150, +200] ms time window were  
263 removed. Only trials in which the response was correct were kept. Event-related potentials (ERPs)  
264 were averaged separately for each subject and for each face orientation (upright, inverted). ERP  
265 subject averages were then grand-averaged separately across the subjects with left-face

266 presentation, and across the subjects with right-face presentation. Significant differences between  
267 the ERP amplitude in the upright versus inverted conditions were detected (separately within the  
268 left-presentation group and the right-presentation groups) using paired t-tests (one-tailed, threshold  
269 at 0.05, to test the hypothesis that upright faces elicit a signal of larger amplitude than inverted  
270 faces) in a clustering procedure (Oostenveld et al., 2011), with a minimum cluster size threshold  
271 of 5 (Scholl et al., 2014). This clustering analysis was performed on all the trials, combining both  
272 eccentricity conditions to increase the signal-to-noise ratio. We ran the analysis on the [0-150ms  
273 time window], i.e., during the stimulus presentation. Signals were selected over the most posterior  
274 channels ( $n = 51$ ), that broadly overlaid posterior visual areas.

#### 275 Experiment 4: fMRI

276 **Participants.** 16 healthy, right-handed human subjects (5 women,  $20.54 \pm 1.1$  years old) with  
277 normal or corrected-to-normal vision took part in the experiment. Three subjects were excluded  
278 from the group analysis: one was singing in the scanner and unable able to focus, the other  
279 turned out to be under medication (Truvada), the third one had an excessive amount of head  
280 motion ( $> 8\text{mm}$ ).

#### 281 Experimental design

282 **Procedure.** In the main experiment, stimuli consisted of natural grayscale scenes (the same as in  
283 the experiments 1 and 2, 50 different scenes) on which 4 items were pasted (height  $2^\circ$ , at  $7^\circ$   
284 eccentricity, at  $25^\circ$  and  $45^\circ$  above and below the horizontal meridian), to match the location and  
285 size of the items in Experiment 1. The items were pasted on gray circles of  $4.5^\circ$  diameter to reduce  
286 the effect of variations in the scene content on the BOLD response. Within an image, the four  
287 items consisted of an upright item (U), the inverted version of U (I), the scrambled version of U

288 (US), the inverted version of US (IS). U was either a face (50 different photograph of faces, chosen  
289 from the same set as in Experiments 2 and 3), or a house (25 different photographs of houses, from  
290 an online database) (Figure 4A). The arrangement of the items U, I, IS, US on the four gray circles  
291 (top left, top right, bottom left, bottom right) was varied across trials, thereby defining four  
292 configurations. The scrambling procedure to create the scrambled items was the one introduced by  
293 Stojanoski & Cusack, 2014, which keeps low-level properties of the items: a degree of warping of  
294 35 was used in order to make the face category unrecognizable. Each participant viewed a total of  
295 four blocks (125 trials per block, 25 faces \* 4 spatial configurations, plus 25 houses). The sets of  
296 faces and houses were repeated twice during the experiment, between two blocks, randomized  
297 between subjects. Within one block, the 25 house trials had the same spatial configuration, with a  
298 different spatial configuration between each block.

299  
300 **Main experiment.** The purpose of the experimental design in this experiment was to mask the  
301 faces and made them invisible to the participants. Each trial (Figure 4B) started with a white  
302 fixation cross on a gray background that was displayed for 1000 ms and was followed by a stream  
303 of 12 characters pseudo-randomly chosen from a set containing the letters of the alphabet, the  
304 numbers 1-9, and 10 punctuation marks ({!, @, #, \$, %, ^, &\*, (, )}), and presented in a rapid  
305 sequence (5 frames each, 60Hz refresh rate) (adapted from (Beck & Kastner, 2005)). In each trial,  
306 a natural scene (with face items or house items, as described above) was embedded in the stream  
307 and stayed on the screen for 4 frames. In 70% of the trials, there was an ‘L’ in the stream. Subjects  
308 were instructed to press a button as soon as they saw the letter ‘L’. The rapid serial visual  
309 presentation aimed at keeping the attention maximally engaged on the center of the screen. The  
310 letter ‘L’ was always displayed after the natural scene so that subjects were fully focused on the

311 letter stream at the moment of appearance of the natural scene. The precise timing of the  
312 presentation of the stimuli of interest (the natural scene with four faces/four houses) was chosen  
313 randomly, it occurred between the 4th to 8th character and could thus not be predicted. Subjects  
314 were instructed to keep their gaze and attention on the stream of characters in the middle of the  
315 screen. They were told that the natural scenes displayed were irrelevant to the task.

316

317 ***MRI acquisition parameters.*** Data were acquired with a 3T MRI scanner (Magnetom Trio,  
318 Siemens) at Georgetown University's Center for Functional and Molecular Imaging. A 12-channel  
319 head coil was used, TR = 2040 ms, TE= 29ms, flip angle = 90°, 35 interleaved axial (thickness =  
320 4.0 mm, no gap; in-plane resolution =  $3.2 \times 3.2 \text{ mm}^2$ ). At the end, 3D T1-weighted MPRAGE  
321 images (resolution  $1 \times 1 \times 1 \text{ mm}^3$ ) were acquired from each participant. Visual stimuli were back-  
322 projected from a computer screen (resolution: 768\*1024) on a mirror within the scanner (distance  
323 mirror-eyes: 89 cm). Data from four runs of event-related scans, one run of face localizer scan,  
324 and two runs of retinotopic localizer scans were acquired from each participant.

325

326 ***V1 retinotopic localizer scans.*** The V1 localizer scans aimed at identifying the portions of V1 (4)  
327 activated by presentation of the faces and houses, in order to focus our analyses on those regions.  
328 High-contrast achromatic flickering (contrast-reversing at 20Hz) checkerboard patterns were  
329 displayed on a gray background (diameter,  $3^\circ$ ) successively at the 4 positions occupied by the  
330 pasted items (top: left and right; bottom: left and right, at  $7^\circ$  eccentricity). The checkerboards were  
331 displayed for 16 consecutive secs at each position and each position was repeated twice. During  
332 the presentation of the checkerboards, in the middle of the screen, the letters 'T' and 'L' were  
333 displayed in alternation, in a randomized order (50 ms of presentation per letter, frequency of

334 occurrence of the letter L: 70%). Similar to the main experiment, subjects were instructed to press  
335 a button every time they were seeing the letter ‘L’. The first retinotopic localizer scan was run  
336 right before the main experiment, the other scan was run right after the main experiment.

337

338 **Face localizer scan.** After the second retinotopic localizer scan, a face localizer scan was run to  
339 identify the Fusiform Face Area (FFA) in each subject. We used stimuli and a similar design as  
340 described in (Kanwisher et al., 1997): 50 different grayscale images of faces and houses, distinct  
341 from the ones in the main experiment, were displayed in the center of the screen in blocks on a  
342 uniform background. Each block, either with faces or with houses, was run twice. The face and  
343 house images were purchased from a commercial source and post-processed using programs  
344 written in MATLAB (The Mathworks, MA) to eliminate background and to adjust image size (to  
345 200 \* 200 pixels), luminance and contrast. 10 subjects were instructed to passively view the  
346 stimuli, 3 others were engaged in a 1-back task to increase attentional engagement.

347 Statistical Analyses

348 **Behavioral Data Analysis.** We computed the signal detection theoretic (SDT) measures  $d'$  and  $c$   
349 (MacMillan & Creelman, 2005) in the target letter detection task. The variable  $d'$  is a measure of  
350 a participant stimulus discrimination sensitivity (here, between the letter ‘L’ and other symbols),  
351 while  $c$  is a measure of a participant bias to report the letter ‘L’. These measures were calculated  
352 on the basis of the rate of hits (letter ‘L’ reported in trials in which the letter ‘L’ was present) and  
353 false alarms (letter ‘L’ reported in trials in which the letter ‘L’ was absent).

354

355 **MRI Data Analysis.** All processing and most statistical analyses were done using the SPM8  
356 software package (<http://www.fil.ion.ucl.ac.uk/spm/software/spm8/>). The first five volumes of

357 each scan were discarded to allow for scanner equilibration. The functional scans and the localizer  
358 scans were preprocessed separately. The echoplanar images (EPIs) were reoriented, then  
359 temporally corrected to the middle slice, spatially realigned, and normalized to the Montreal  
360 Neurological Institute (MNI) template brain. Images were then smoothed with a full-width at half-  
361 maximum of 6 mm Gaussian kernel. After removing low-frequency temporal noise with a high-  
362 pass filter (1/128 Hz), fMRI responses were modeled with a design matrix comprising the onset  
363 of trial types and movement parameters as regressors using a standard hemodynamic response  
364 function.

365

366 ***Identification of V1 Regions of interest (ROIs).*** V1 regions of interest were identified from the  
367 two retinotopic localizer scans, separately for each participant, via the MarsBar toolbox (Brett et  
368 al., 2002). Participant-specific ROIs were identified with the contrast of one checkerboard position  
369 versus the three other checkerboard positions and this was performed for each of the 4 positions.  
370 Each contrast resulted in a focus located in the contralateral hemisphere, below the calcarine sulcus  
371 (CS) for checkerboards presented in the upper visual field, and above the CS for checkerboards  
372 presented in the lower visual field. We could infer from (Dougherty et al., 2003) that each  
373 checkerboard (diameter: 3°, at 7° eccentricity) should activate around 75 mm<sup>3</sup> of cortical surface in  
374 V1, i.e. approximately 10 voxels of 8 mm<sup>3</sup>. Based on this estimation, to define V1 ROI, we  
375 adjusted the statistical threshold to obtain, in each participant, clusters of approximately 10-15  
376 voxels (significant at the corrected cluster level of at least  $p < 0.05$ , else, at the uncorrected cluster  
377 level of at least  $p < 0.001$ ) (Glezer et al., 2015, Jiang et al., 2006). We thus aimed at identifying  
378 V1 ROIs, through the use of checkerboard stimuli which are known to strongly activate V1 (Engel  
379 et al., 1997), and by restricting the ROIs to 15 voxels. However, for reasons of parsimony, because

380 the activity in V1 propagates to V2, we interpret our data as being in V1/V2, in other words in the  
381 early visual cortex.

382

383 ***Identification of face-selective ROIs.*** Face-selective ROIs were identified from the localizer scan  
384 separately for each participant, via the MarsBar toolbox (Brett et al., 2002). Epochs with face and  
385 house stimuli were modeled with two box-car functions convolved with a canonical hemodynamic  
386 response function (HRF). Participant-specific ROIs were defined by voxels that displayed face >  
387 house responses. We focused our analysis on the right FFA (Kanwisher et al., 1997, Jiang et al.,  
388 2006). ROIs were selected by identifying in each participant the cluster in the right temporal cortex  
389 that was significant at the cluster level (corrected cluster level, at least  $p < 0.05$  else, uncorrected  
390 cluster level, at least  $p < 0.001$ ). With such thresholds, only subjects for whom a cluster of at least  
391 30 voxels was found, in a location close to the published location of the right FFA, approximate  
392 MNI coordinates ( $39 \pm 3$   $-40 \pm 7$   $-16 \pm 5$ ) (Grill-Spector et al., 2002) were included in the FFA  
393 analysis ( $n = 8$  out of 13). In 3 out of the 5 subjects for which no right FFA-cluster could be found  
394 with the contrast face > house, we could obtain, through the contrast face > baseline, a right FFA-  
395 cluster in a location close to the published location of the right FFA according to Grill-Spector et  
396 al., 2002. Analyses were run within the homogenous set of 8 subjects whose FFA was defined via  
397 the contrast face > house, and, to increase the statistical power, analyses were also run with the 3  
398 additional subjects with the cluster found via the contrast face > baseline.

399

## 400 Results

### 401 Experiment 1: Fast saccades toward faces have limited selectivity

402 We asked subjects to saccade, as fast as they could, toward faces in natural scenes containing a  
403 face as well as a distractor sharing, to different degrees, physical properties with faces.

404 The comparison of the percentage of saccades oriented toward the face versus the distractor  
405 revealed that, when the distractor was a configuration-scrambled face (i.e., a face whose internal  
406 parts had been scrambled randomly, see Figure 1 A), subjects made as many saccades toward the  
407 configuration-scrambled face as toward the target face (Figure 1B), despite the instruction to  
408 saccade toward the normal face (% saccades in the quadrant with the normal face:  $40.31\% \pm$   
409  $1.72\%$ , with a configuration-scrambled face:  $42.93\% \pm 2\%$ , paired t test:  $T_{(7)} = -1.18$ ,  $p = 0.27$ ). In  
410 trials with an inverted face, a phase-scrambled face or a house, subjects made more saccades  
411 toward the face than toward the distractor (inverted face distractors: % saccades in the quadrant  
412 with the face:  $49.28\% \pm 2.1\%$ , with an inverted face:  $34.63\% \pm 1.67\%$ ,  $T_{(7)} = 6.6$ ,  $p = 3 * 10^{-4}$ ;  
413 house distractors: % saccades in the quadrant with the face:  $68.35\% \pm 3.35\%$ , house distractors:  
414  $14.9\% \pm 0.7\%$ ,  $T_{(7)} = 13.89$ ,  $p = 2 * 10^{-6}$ ; phase-scrambled distractors: with the face:  $65.92\% \pm$   
415  $3.53\%$ , with a phase-scrambled face:  $16.06\% \pm 1\%$ ,  $T_{(7)} = 11.9$ ,  $p = 6 * 10^{-6}$ ). The min SRT, a  
416 statistical estimate of the latency at which the first saccades to the (target) face start to be more  
417 numerous than toward the distractor (Material and Methods), were, on average,  $140 +22$  ms,  $149$   
418  $\pm 7$  ms,  $136 \pm 11$  ms,  $138 \pm 15$  ms (in the configuration-scrambled, inverted face, phase-scrambled,  
419 house distractor conditions, resp.). Note that minimum SRTs in this experiment were longer than  
420 in Crouzet et al., 2010, presumably since subjects expected the distractors to be similar to the target  
421 and therefore potentially adopted a more cautious strategy.

422

423 Since saccades to faces have been found to be more accurate and faster when the faces were  
424 displayed in the left visual field rather than in the right visual field (Crouzet et al., 2010), we  
425 conducted a separate analysis of the saccades when the face and the distractor were both in the left  
426 hemifield versus both in the right hemifield. In trials with an inverted face distractor, a higher  
427 number of saccades toward the face relative to the distractor was observed for left-hemifield  
428 presentation of the face and distractor (% saccades within the quadrant with the face:  $51\% \pm 1\%$ ,  
429 with an inverted face:  $38.6\% \pm 1\%$ ,  $T_{(7)} = 5.24$ ,  $p = 0.001$ ). In contrast, for right-hemifield  
430 presentation of the face and distractor, subjects made saccades as often toward the inverted face as  
431 toward the upright target face (% saccades within the quadrant with the face: 41%, with an inverted  
432 face: 36%, paired t test:  $T_{(7)} = 0.84$ ,  $p = 0.42$ ) (Figure 1C), suggesting lower face selectivity for  
433 right-hemifield presentations. For the other categories, we did not expect such an asymmetry  
434 because configuration-scrambled faces act as perfect distractors while houses and phase-scrambled  
435 faces do not act as effective distractors.

436

437 In summary, Experiment 1 provided evidence that fast face detection has limited shape selectivity,  
438 with configuration-scrambled faces frequently being mistaken for targets. This finding is  
439 compatible with the notion of fast face detection being based on detectors that encode only face  
440 parts, not holistic faces. Supporting this hypothesis, inverted faces, whose parts are affected  
441 somewhat by inversion, were not as effective distractors as the configuration-scrambled faces.  
442 Another interesting finding from Experiment 1 was a hemispheric asymmetry of fast face  
443 detection, with an advantage for face detection in the left visual hemifield. We next conducted

444 another experiment to more finely assess the spatial precision as well as lateralization effects of  
445 the earliest saccades oriented toward faces.

446 Experiment 2: Faces are saccaded to faster and more precisely when they are in the  
447 left hemifield

448 In Experiment 2, subjects were asked to detect faces in “annulized” natural images consisting of a  
449 natural scene windowed by an annulus, which contained a face image ( $2^\circ$  of visual angle high).  
450 The saccades started as early as 100-120 ms post stimulus onset (Figure 2C). Figure 2B shows that  
451 saccades were aggregated in an area centered on the faces and extending up to about 15-20 polar  
452 degrees on both sides. We therefore labeled as “correct” the saccades that landed in an area  
453 centered on the faces and extended up to 15 degrees both sides and computed the minSRT  
454 (Material and Methods). The correct saccades represented  $59.6 \pm 4\%$  of the total number of  
455 saccades and landed at  $1.07^\circ \pm 0.05^\circ$  visual angle from the center of the face, with an average  
456 latency of 182.3 ms (average of the moment of onset of the first saccades). The minimum SRT  
457 (Material and Methods) was shorter for left presentations than for right presentations (minimal  
458 SRT, on average, left-presentation:  $160 \pm 4$  ms, right presentation:  $177 \pm 4$  ms, paired t-test,  $T_{(15)}$   
459  $= -3.2$ ,  $p = 0.008$ ) (Figure 2C). Furthermore, saccades landed closer to the face in left-presentation  
460 trials relatively to right-presentation trials (left presentation:  $3.54^\circ \pm 0.28^\circ$ , right presentation:  $4.06$   
461  $^\circ \pm 0.25^\circ$ , paired t-test:  $T_{(15)} = -2.8$ ,  $p = 0.013$ ).

462

463

464 Experiment 3: EEG data reveal face-specific responses 40 to 110 ms post-stimulus  
465 onset for left-hemifield presentations

466 To probe the neural bases of fast face localization, we conducted a high-density  
467 electroencephalography (EEG) study and assessed the earliest latency of face-selective neural  
468 signals. We presented faces in the periphery while asking subjects to look at a central fixation spot  
469 and perform an upright/inverted face classification task on peripherally presented faces. They were  
470 presented on one side of the screen only, with presentation side alternating between subjects. Akin  
471 to previous studies of higher-level face processing (Kanwisher et al., 1998 ; Rossion et al., 2000),  
472 and motivated by the observation of an advantage for upright vs. inverted faces in fast face  
473 detection (Experiment 1), we adopted a stringent test to establish face selectivity of neural  
474 responses, requiring significantly different neural responses to upright vs. inverted faces. This  
475 contrast avoids confounds arising from low-level stimulus differences between faces and  
476 comparison objects (e.g., when comparing responses to faces versus houses, which can be  
477 differentiated by other low-level features such as different luminance distributions). To engage  
478 attention to the faces, as in (Rossion & Caharel, 2011), we engaged subjects in a face categorization  
479 task (upright vs. inverted).

480 Reaction times in the upright/inverted face categorization tasks were computed on the trials kept  
481 for the EEG analysis, i.e., on the correct trials. Across the 10 subjects whose eye movements were  
482 recorded,  $11.7 \pm 2.8$  % of the trials on average were aborted due to eye movements. Subjects were  
483 faster responding to upright faces than inverted faces (paired t-test, mean average reaction time for  
484 correct trials, left-presentation group, upright faces:  $538 \pm 28.3$  ms, inverted faces:  $586 \pm 35$  ms,  
485  $T_{(8)} = -3.6$ ,  $p = 0.0069$ ; right-presentation group, upright faces:  $603 \pm 48$  ms, inverted faces:  $651 \pm$   
486  $48.5$  ms,  $T_{(9)} = -4.4$ ,  $p = 0.0016$  ; note that these reaction times were substantially longer than the

487 0-100ms time window of interest). Reaction times were not significantly different between the  
488 left- and right-presentation groups (unpaired t-test:  $T_{(18)} = -1.05$ ,  $p = 0.3$ ). Accuracy was very high,  
489 and similar between the groups (unpaired t-test, mean accuracy, left-presentation group:  $93.3 \pm$   
490  $1\%$ , right-presentation group:  $91.3 \pm 2.5\%$ ,  $T_{(18)} = 0.72$ ,  $p = 0.47$ ). The average number of trials  
491 kept for the EEG analysis was similar in the left- and in the right-presentation groups (unpaired t-  
492 test, left-presentation group:  $705 \pm 43$  trials, right-presentation group:  $625 \pm 27$  trials,  $T_{(18)} = 1.6$ ,  
493  $p > 0.1$ ).

494

495 A clustering analysis was done using Fieldtrip (Oostenveld et al., 2011) between 0-150 ms  
496 relatively to stimulus onset over the most posterior channels, which capture (early) visual-evoked  
497 responses and notably V1 activity (Foxe & Simpson, 2002). In the left-presentation group, a  
498 significant cluster ( $p = 0.035$ ) differentiating the signal in the upright and inverted conditions  
499 between 40 and 110 ms was found (Figure 3A). The cluster was lateralized in the right hemisphere  
500 (Figure 3B). In the right-presentation group, the cluster started later, extending from 98 to 140 ms  
501 ( $p = 0.04$ ) (Figure 3C). The cluster was initially lateralized in the left hemisphere (Figure 3D). A  
502 control analysis was run to verify that the early clusters with a significantly higher signal amplitude  
503 for upright vs. inverted faces were not driven by subjects without eye recordings, who could have  
504 moved their eyes despite the instruction not to do so. Specifically, we computed the mean signal  
505 amplitude for each condition (upright and inverted configurations) within the subjects whose eye  
506 movements were recorded. We predicted that for participants whose eye movements were  
507 recorded and who maintained fixation throughout each trial (Material and Methods), thus with no  
508 possible contamination of the ERP by eye movements, we should observe a significant difference  
509 between the upright vs. inverted conditions in the ERP. In this analysis, we combined the

510 participants with left-hemifield and right-hemifield presentation in order to increase statistical  
511 power. This analysis revealed that the differences were indeed observed within those subjects  
512 (group of subjects with eye movements recorded, within the appropriate cluster according to the  
513 presentation side, upright condition:  $1.16 \pm 0.36$ , inverted condition:  $0.87 \pm 0.32$ ,  $T_{(10)} = 3.9$ ,  $p =$   
514  $0.0029$ ). This confirms that the early face selectivity could not be explained by differential  
515 movements toward upright versus inverted faces.

516

#### 517 Experiment 4: fMRI data provide evidence for face-specific responses in V1/V2

518 To identify the sources of the early face-selective neural signal, we conducted an fMRI study.  
519 Subjects were engaged in a central letter detection task during a rapid serial visual presentation  
520 (RSVP) of symbols and letters, while small faces and houses ( $2^\circ$ ) were displayed in the periphery  
521 ( $7^\circ$ ). In the central letter detection task, subjects had, on average, a high  $d'$ -prime that stayed stable  
522 across blocks, thus suggesting that they stayed engaged over the whole duration of the experiment  
523 (across the four blocks, mean,  $d' = 3.3$ , mean criterion  $c: -0.8$ ; repeated-measures ANOVA over  
524 criterion  $c$  with the single factor Block,  $F_{(1, 12)} = 2.05$   $p = 0.12$ ). Debriefing at the end of the  
525 experiment revealed that none of the subjects noticed either faces or houses items.

#### 526 V1-response to the face stimuli from different categories

527 We used upright faces (U), inverted faces (I), scrambled upright (US) and scrambled inverted (IS)  
528 faces in order to probe for face selectivity in V1. Similarly to the EEG Experiment (Experiment  
529 3), we used inverted faces to assess face selectivity. We also used scrambled faces as a control.  
530 The scrambling procedure (from Stojanoski & Cusack, 2014, described in the Methods section)  
531 preserved the faces' basic visual properties, to which the earliest stages of the visual processing

532 are sensitive, while making faces unrecognizable as faces. We reasoned as follows: if there is some  
533 selectivity to faces in V1, the BOLD signal in response to U faces should be higher than for the  
534 other three categories. The contrast {US vs. IS} enabled us to check that a differential BOLD  
535 signal between U versus I items does not arise from an inversion effect but is truly a response  
536 specific to upright faces.

537

538 Retinotopic localizer scans with flickering checkerboards known to evoke strong responses in V1  
539 (Engel et al., 1997) were used to define the regions of V1 activated during the functional runs by  
540 our visual stimulation in periphery (4 items pasted at 7° eccentricity, see Figure 4A). The four  
541 ROIs were in the lower and upper bank of the left and right calcarine sulcus, corresponding to the  
542 upper and lower presentation of the checkerboards respectively (Material and Methods, mean  
543 coordinates of the ROIs: activated by top left presentations:  $(12 \pm 1 \ -78 \pm 1 \ -5 \pm 1)$ , bottom left:  
544  $(12 \pm 1.1 \ -92 \pm 1 \ 21 \pm 2)$ , top right:  $(-10 \pm 1 \ -81 \pm 1.3 \ -8 \pm 1.2)$ , bottom right:  $(-8 \pm 1 \ -97 \pm 1 \ 16 \pm$   
545  $2)$ ). The ROI subtended approximately 15 voxels (mean size of the ROI:  $13.9 \pm 0.68$ , activated by  
546 top left presentations:  $13.07 \pm 0.67$ , bottom left presentations:  $12.08 \pm 0.53$ , top right presentations:  
547  $14.2 \pm 0.94$ , bottom right presentations:  $16.15 \pm 2.5$ , repeated-measures ANOVA over the ROIs  
548 size, factor ROI location:  $F_{(1,12)} = 0.13$ ,  $p = 0.25$ ).

549

550 We first considered the percent signal change collapsed across the four ROIs. Responses in V1/V2  
551 to upright and inverted faces were similar, regardless of scrambling status: the unscrambled faces  
552 (mean % signal change, U:  $0.34 \pm 0.04$ , I:  $0.33 \pm 0.04$ , paired t-test,  $T_{(12)} = 1.6$ ,  $p = 0.13$ ), and the  
553 scrambled faces (mean % signal change, US:  $0.33 \pm 0.04$ , IS:  $0.33 \pm 0.04$ , paired t-test,  $T_{(12)} = -$   
554  $0.0026$ ,  $p = 0.99$ ). A repeated-measures ANOVA on percent signal change showed that the

555 amplitude of the percent signal change in the V1 ROIs was similar between the scrambled and the  
556 unscrambled pairs (main effect, factor Orientation (upright/inverted):  $F_{(1, 12)} = 0.028$ ,  $p = 0.87$ ,  
557 factor Scrambling (scrambled/unscrambled):  $F_{(1, 12)} = 0.69$ ,  $p = 0.42$ , interaction Orientation x  
558 Scrambling:  $F_{(1, 12)} = 0.87$ ,  $p = 0.37$ ).

559

560 Next, based on the lateralization effects found in behavior and EEG, we analyzed the BOLD  
561 contrast responses by hemifield (mean size of the two ROIs from left presentations:  $12.69 \pm 0.61$ ,  
562 of the two ROIs from right presentations:  $15.19 \pm 1.9$ , paired t-test,  $T_{(12)} = -1.7$ ,  $p = 0.1$ ).  
563 Interestingly, in the right hemisphere ROIs (activated by left hemifield presentations), the percent  
564 signal change in response to upright faces was significantly higher than to inverted faces for  
565 unscrambled faces (mean % signal change, U:  $0.35 \pm 0.036$ , I:  $0.34 \pm 0.04$ , paired t-test,  $T_{(12)} =$   
566  $3.19$ ,  $p = 0.0077$  (Figure 4C), with 10 out of 13 subjects with a higher percent signal change for  
567 the upright face trials) (Figure 4D, left). In contrast, for scrambled faces, responses to upright  
568 versus inverted stimuli was similar (mean % signal change, US:  $0.33 \pm 0.036$ , IS:  $0.34 \pm 0.039$ ,  
569 paired t-test,  $T_{(12)} = -0.8$ ,  $p = 0.43$ , with 6 out of 13 subjects with a higher percent signal change  
570 for the upright scrambled face trials (Figure 4D, right)). There also was no significant difference  
571 between the response to I and IS ( $T_{(12)} = 0.63$ ,  $p = 0.53$ ), nor between the response to I and US, as  
572 predicted ( $T_{(12)} = 0.17$ ,  $p = 0.86$ ). By contrast, when the analysis was restricted to the left  
573 hemisphere ROIs (activated by right hemifield presentations), no significant difference between  
574 the percent signal change to upright versus inverted faces was found in V1/V2, neither for the  
575 unscrambled faces (mean % signal change, U:  $0.32 \pm 0.041$ , I:  $0.32 \pm 0.043$ , paired t-test,  $T_{(12)} =$   
576  $-0.75$ ,  $p = 0.46$ ), nor for the scrambled faces (mean % signal change, US:  $0.33 \pm 0.045$ , IS:  $0.32$   
577  $\pm 0.044$ , paired t-test,  $T_{(12)} = 0.55$ ,  $p = 0.58$ ) (Figure 4E). We performed a repeated-measures

578 ANOVA on percent signal change, with factors Orientation and Scrambling to check whether there  
579 was a difference in the BOLD-signal for U vs. I faces that was specific to the unscrambled faces.  
580 This ANOVA, when performed for left-hemifield presentation, confirmed that the response to  
581 upright versus inverted faces was different between the scrambled and the unscrambled conditions  
582 (main effect, factor Orientation (upright/inverted):  $F_{(1, 12)} = 0.6$ ,  $p = 0.43$ , factor Scrambling  
583 (scrambled/unscrambled):  $F_{(1, 12)} = 0.97$ ,  $p = 0.34$ , interaction Orientation x Scrambling:  $F_{(1, 12)} =$   
584  $4.36$ ,  $p = 0.05$ ). By contrast, for right-hemifield presentation, the response to upright versus  
585 inverted faces was similar between the scrambled and the unscrambled conditions (main effect,  
586 factor Orientation (upright/inverted):  $F_{(1, 12)} = 1.18$ ,  $p = 0.29$ , factor Scrambling  
587 (scrambled/unscrambled):  $F_{(1, 12)} = 0.014$ ,  $p = 0.9$ , interaction Orientation x Scrambling:  $F_{(1, 12)} =$   
588  $0.75$ ,  $p = 0.41$ ). This difference between the left versus right presentation paralleled the findings  
589 in behavior (Experiments 1 and 2) and EEG (Experiment 3).

590

591 To avoid saccades, we flashed the stimuli very briefly (67 ms), a time too short for eye movements  
592 to the stimuli of interest since express saccades, the fastest oriented-saccades in humans, peak at  
593 100 ms (Fischer & Ramsperger, 1984). Furthermore, the debriefing showed that subjects were  
594 unaware of the presence of faces in the trials. It is therefore unlikely that the difference in the  
595 percent signal change between trials with upright and inverted faces (left hemifield presentations,  
596 unscrambled faces) reflected differential patterns in eye movements. Additionally, if eye  
597 movements toward peripheral items drove this effect, we would expect that the higher the effect  
598 size in the BOLD signal was, the worse the accuracy should have been in the central task. Yet, no  
599 correlation was found between the effect size in the BOLD signal (computed as the contrast in  
600 percent signal change to I vs. U, analysis restricted to left hemifield presentations) and behavior,

601 both when considering the  $d'$ -measure (Pearson correlation,  $r = 0.34$ ,  $p = 0.25$ ), or when  
602 considering the criterion (Pearson correlation,  $r = 0.32$ ,  $p = 0.28$ ).

603

604 The FFA is known to exhibit a larger BOLD signal in response to faces than to houses (Liu et al.,  
605 2002). Therefore, we performed a control analysis in the FFA ROIs in order to check whether the  
606 differential response in V1/V2 ROIs to upright vs. inverted faces presentations could be due to a  
607 differential response to upright versus inverted faces in the FFA, that would feed back to early  
608 visual areas. The right FFA could be identified in 8 participants through the contrast face > house  
609 (mean coordinates:  $(43 \pm 1.41 -49 \pm 2.44 -20 \pm 2.07)$ , mean size:  $103.3 \pm 22.81$  voxels).  
610 Interestingly, while, in the localizer scans, the FFA ROIs were identified via the higher BOLD-  
611 signal for face presentations relatively to house presentations, in the functional scans that included  
612 the flashed peripheral presentation of small faces and houses (Material and Methods for details),  
613 no significant difference was observed in the percent signal change between face and house  
614 presentation trials (mean percent signal change in face trials:  $0.27 \pm 0.025$ , in house trials:  $0.27 \pm$   
615  $0.034$ , paired t-test,  $T_{(7)} = 0.13$ ,  $p = 0.89$ ). There was no significant difference either between the  
616 percent signal change in face trials split by the hemifield of presentation of the unscrambled faces,  
617 to which the FFA is usually responsive (mean percent signal change, unscrambled faces on the  
618 left:  $0.26 \pm 0.027$  on the right:  $0.28 \pm 0.02$ , paired t-test,  $T_{(7)} = -0.84$   $p = 0.42$ ). To test the  
619 robustness of these null effects, we ran the same analysis while adding three more participants ( $n$   
620 = 11 out of 13) for which an FFA-cluster could be identified when using the contrast face > baseline  
621 (across the 11 participants, mean Talairach coordinates:  $(40.9 \pm 1.58 -52.7 \pm 3.41 -19.45 \pm 1.77)$ ,  
622 mean size:  $93.9 \pm 17.21$  voxels). Adding those three participants did not change the results – no  
623 significant difference was found in trials with faces versus houses (mean percent signal change, in

624 face trials:  $0.27 \pm 0.018$ , in house trials:  $0.28 \pm 0.028$ , paired t-test,  $T_{(10)} = -0.38$ ,  $p = 0.7$ ), and no  
625 difference between trials with faces on the left versus on the right hemifield (mean percent signal  
626 change, unscrambled faces on the left:  $0.27 \pm 0.02$  on the right:  $0.28 \pm 0.013$ , paired t-test,  $T_{(10)} =$   
627  $-0.68$   $p = 0.5$ ). Thus, in our experiment, the small, peripherally presented faces did not elicit face-  
628 specific activation in the FFA.  
629

## 630 Discussion

631 In the present study, motivated by the remarkably short latency and high localization accuracy of  
632 fast saccades to faces, we investigated the hypothesis that the early visual cortex contains selective  
633 neural representations for complex objects of high ecological importance, specifically faces.  
634 Experiment 1 showed that, compatible with a location in lower visual areas, the specificity of fast  
635 saccades to faces is moderate, with “configuration-scrambled” and inverted faces interfering  
636 substantially with the localization of upright faces. Experiments 1 and 2 also revealed a key  
637 signature of fast saccades to faces, namely an asymmetry between the two hemifields that is  
638 characterized by a higher selectivity for upright vs. inverted faces for left hemifield presentations  
639 (Experiment 1), spatially more accurate and faster saccades for this hemifield (Experiment 2).  
640 Second, an EEG experiment (Experiment 3) revealed that event-related potentials (ERPs)  
641 differentiated between upright and inverted faces in the left hemifield from 40 ms post-stimulus  
642 onset, i.e., in the latency of the first estimated responses in V1 as measured on the scalp (Foxye et  
643 al., 2008). For faces displayed in the right visual hemifield, the earliest significant difference in  
644 the ERPs between upright and inverted faces started later, at 98 ms post-stimulus onset. This  
645 asymmetry between the hemifields in the EEG results therefore matched the asymmetry found in

646 the behavioral experiments. It is worth noting that the EEG difference in latency of the early face-  
647 selective response between the left-presentation and right-presentation groups was larger than the  
648 difference in minimum saccadic reaction times in Experiment 2. However, participants in that  
649 experiment were not only slower for right hemifield presentations but also less accurate. This  
650 speed-accuracy tradeoff suggests that behavioral latency differences did not fully compensate  
651 neuronal latency differences in Experiment 2. Third, an fMRI experiment (Experiment 4) revealed  
652 that in V1/V2, upright faces elicited a higher percent signal change in the BOLD signal than  
653 inverted faces. Again, this face-specific response was found specifically for faces displayed in the  
654 left visual hemifield, but not for faces displayed in the right visual hemifield. Thus, we found a  
655 high degree of agreement between the behavioral, EEG, and fMRI results suggestive of face-  
656 selective neuronal populations in early visual cortex.

657

658 Our results come in the wake of recent reports suggestive of face selectivity in early vision. EEG  
659 classification results indicate that EEG potentials recorded over occipital locations can predict the  
660 location of faces as early as 50ms post-stimulus onset (Martin et al., 2014). In an MEG study, the  
661 authors reported, for left (but notably not right) presentations, larger responses to face-like vs.  
662 house-like patterns in early visual areas with short latencies (Shigihara & Zeki, 2014), but the  
663 comparison of responses across different channel groupings for different stimuli in that study left  
664 open the specificity of the observed effect. A recent ECoG study (Matsuzaki et al., 2015) reported  
665 response differences between upright and inverted faces within 40-90ms following stimulus onset  
666 over early visual areas V1 and V2. However, most of the electrodes (80%) were placed in locations  
667 corresponding to the upper visual field, therefore resulting in different physical stimulation in the  
668 upright face trials versus the inverted face trials. Thus, the differential response might have been

669 elicited by a difference in the physical stimulation. In Uyar et al., 2015, the authors reported a  
670 differential response to faces vs. houses in early visual areas. However, it is problematic to use the  
671 face vs. house contrast as a marker for face selectivity in V1 since a differential response to faces  
672 versus houses can be driven by low-level differences between the two stimulus classes, given the  
673 known selectivity of V1 neurons for low-level features (e.g. luminance, spatial frequency). For  
674 this reason, to provide a more selective probe for face selectivity, our study used inverted faces,  
675 which have been used as a specific control for face processing in a large number of studies (Haxby  
676 et al., 1999 ; Itier & Taylor, 2002 ; Kanwisher et al., 1998). As a further test, we created scrambled  
677 faces that are unrecognizable as faces yet preserve the original faces' low-level properties; we  
678 found that unscrambled inverted faces and scrambled faces in their upright and inverted version  
679 elicited a similar percent BOLD signal change in early visual areas ROIs, lower than the signal  
680 elicited by unscrambled upright faces. This strongly confirms that the response in the early visual  
681 cortex that we found is a response specific to faces as an abstract category, that cannot be accounted  
682 for by low-level properties of faces.

683

684 The left / right asymmetry that we found across the experiments parallels the well-known left  
685 hemifield advantage found for face recognition and categorization (Gilbert & Bakan, 1973,  
686 Rhodes, 1985, Sergent & Bindra, 1981) and the right hemisphere advantage for neural  
687 representation of faces (Yovel et al., 2008). It has been postulated that asymmetries in visual  
688 processing between the left and right hemisphere relate to the level of processing (local vs. global),  
689 spatial frequency content of stimuli, or the visual pathway (magno- vs. parvocellular) (for a review,  
690 see (Hellige, 1996)). While the mechanisms responsible for the face processing asymmetry are  
691 beyond the scope of this paper, it might be of significant interest for future studies to directly

692 investigate the relationship between the low-level face processing asymmetry with the asymmetry  
693 of high-level face processing (e.g., in the FFA).

694

## 695 [A new view of hierarchical processing in the visual system](#)

696 Our study suggests the intriguing hypothesis that there might be neural representations selective  
697 for certain complex object classes (such as faces) at the lowest levels of the visual hierarchy. This  
698 finding challenges the standard simple-to-complex hierarchical description of the visual system  
699 according to which complex object categories are processed at high levels of the visual hierarchy.  
700 It is unlikely that the selectivity in early visual areas for upright faces identified in our study  
701 (Experiment 4) is the result of feedback activity from areas belonging to the core network for face  
702 perception, such as the FFA or the OFA (occipital face area) (Haxby et al., 2000). First, in our  
703 study, the usual contrast of Faces vs. Houses, to which the FFA is normally responsive (Liu et al.,  
704 2002), did not reveal any significant difference of the percent BOLD signal. This might be due to  
705 the fact that the faces were presented in the periphery while the FFA is mostly responsive to central  
706 face presentations (Levy et al., 2001). Second, the debriefing conducted at the end of Experiment  
707 4 indicated that subjects did not notice the presence of faces or houses. Those subjective reports  
708 suggest that the masking was efficient, thus preventing feedback-driven face-specific activity in  
709 V1/V2 (Fahrenfort et al., 2007). Taken together, the early latency of the face-specific response  
710 found in the EEG signals and the localization of the face-specific response in V1/V2 suggest that  
711 face-specific responses emerge during a first forward sweep of processing and truly reflect a  
712 selectivity to faces in early vision rather than the propagation in feedback of the activity from  
713 higher-level areas.

714

715 Given its position at a low level of the visual processing hierarchy, we would not expect that the  
716 degree of face selectivity in V1/V2 would be comparable to the high degree of face selectivity in  
717 the FFA, which has been shown to be involved in the discrimination of different faces identities  
718 (for a review, see Kanwisher et al., 2006). In fact, the observation that the fast saccades were  
719 attracted toward the configuration-scrambled faces (Experiment 1) suggests that face  
720 representations in V1/V2 are not selective for the configuration of the faces, in line with findings  
721 about face representations in higher areas of occipital cortex that are not selective for the face-part  
722 configurations (the Occipital Face Area, OFA) (Pitcher et al., 2007; Liu et al 2010), in contrast to  
723 face representations further downstream in fusiform cortex (Andrews et al., 2010; Liu et al., 2010).  
724

725 The face-specific neural response that we observed in V1/V2, starting at 40 ms post-stimulus onset,  
726 constitutes a likely underpinning for the fast saccadic detection of faces. Such a model of  
727 “shortcuts” in hierarchical visual processing, with early visual representations directly providing  
728 input to decision circuits for fast motor responses is compatible with recent theories of  
729 thalamocortical processing (Sherman, 2016) in which corticofugal projections from layer 5 in early  
730 visual areas could carry task-relevant signals directly to the superior colliculus. It will be very  
731 interesting in future work to explore the plasticity of this circuit, to see whether it is possible to  
732 learn fast saccades for new object classes in addition to faces by effecting object-specific plasticity  
733 in early visual areas.

734

735 **Author contribution**

736 F.C, M.R., X.J., J.G.M., S.J.T designed experiments. F.C. ran experiments with assistance from

737 L.B. F.C. and M.R. analyzed the data. All co-authors contributed to the writing of the manuscript.

## 738 **References**

739

740 Aine, C. J., Suppek, S., George, J. S., Ranken, D., Lewine, J., Sanders, J., & Wood, C. C. (1996).  
741 Retinotopic organization of human visual cortex: departures from the classical model. *Cerebral*  
742 *Cortex*, 6(3), 354-361.

743 Andrews, T.J., Davies-Thompson, J., Kingstone, A., and Young, A.W. (2010). Internal and  
744 External Features of the Face Are Represented Holistically in Face-Selective Regions of Visual  
745 Cortex. *J. Neurosci.*, 30(9), 3544–3552.

746 Beck, D.M., and Kastner, S. (2005). Stimulus context modulates competition in human extrastriate  
747 cortex. *Nat. Neurosci.*, 8(8), 1110–1116.

748 Brett, M., Anton, J. L., Valabregue, R., & Poline, J. B. (2002). Region of interest analysis using  
749 an SPM toolbox. 8th international conference on functional mapping of the human brain (Vol.  
750 16, No. 2, p. 497).

751

752 Brillhault, A., Mathey, M., Jolmes, N., & Thorpe, S. J. (2011). Measuring the receptive field sizes  
753 of the mechanisms underlying ultra-rapid saccades to faces. *Perception ECVF abstract*, 40, 157-  
754 157.

755

756 Cauchoix, M., Barragan-Jason, G., Serre, T., & Barbeau, E. J. (2014). The neural dynamics of  
757 face detection in the wild revealed by MVPA. *J. Neurosci.*, 34(3), 846-854.

758 Crouzet, S.M., Thorpe, S.J. (2010). Fast saccades toward faces : Face detection in just 100 ms. *J*  
759 *Vis.*, 10(4), 1–17.

- 760 Crouzet, S. M., & Thorpe, S. J. (2011). Low-level cues and fast face detection. *Frontiers in*  
761 *psychology*, 2, 342.
- 762 Delorme, A., & Makeig, S. (2004). EEGLAB: an open source toolbox for analysis of single-trial  
763 EEG dynamics including independent component analysis. *J. Neurosci. Methods*, 134(1), 9-21.
- 764 Di Russo et al. (2005). Identification of the neural sources of the pattern-reversal  
765 VEP. *NeuroImage*, 24(3), 874-886.
- 766 Dougherty, R. F., Koch, V. M., Brewer, A. A., Fischer, B., Modersitzki, J., & Wandell, B. A.  
767 (2003). Visual field representations and locations of visual areas V1/2/3 in human visual  
768 cortex. *J. Vis.*, 3(10), 1-1.
- 769 Dumoulin, S.O., Wandell, B.A. (2008). Population receptive field estimates in human visual  
770 cortex. *Neuroimage*, 39(2), 647-660.
- 771 Eimer, M., Gosling, A., Nicholas, S., & Kiss, M. (2011). The N170 component and its links to  
772 configural face processing: a rapid neural adaptation study. *Brain research*, 1376, 76-87.
- 773 Engel, S. A., Glover, G. H., & Wandell, B. A. (1997). Retinotopic organization in human visual  
774 cortex and the spatial precision of functional MRI. *Cerebral cortex*, 7(2), 181-192.
- 775
- 776 Fabre-Thorpe, M., Delorme, A., Marlot, C., & Thorpe, S. (2003). A limit to the speed of processing  
777 in ultra-rapid visual categorization of novel natural scenes. *J. Cogn. Neurosci.*, 13(2), 171-180.
- 778
- 779 Fahrenfort, J. J., Scholte, H. S., & Lamme, V. A. (2007). Masking disrupts reentrant processing  
780 in human visual cortex. *J. Cogn. Neurosci.*, 19(9), 1488-1497.

- 781 Fischer, B., Ramsperger, E. (1984). Experimental Brain Research Human express saccades:  
782 extremely short reaction times of goal directed eye movements. *Exp. Brain. Res.*, 57, 191–195.
- 783 Fischer, B., Weber, H. (1993). Express saccades and visual attention. *Behav. Brain Sci.*, 16(3),  
784 553-567.
- 785 Foxe, J.J., Simpson, G. (2002). Flow of activation from V1 to frontal cortex in humans. *Exp. Brain*  
786 *Res.*, 142(1), 139–150.
- 787 Foxe, J.J., Strugstad, E.C., Sehatpour, P., Molholm, S., Pasioka, W., Schroeder, C.E., McCourt,  
788 M.E. (2008). Parvocellular and magnocellular contributions to the initial generators of the visual  
789 evoked potential: High-density electrical mapping of the “C1” component. *Brain Topogr.*, 21(1),  
790 11–21.
- 791 Gilbert, C., & Bakan, P. (1973). Visual asymmetry in perception of  
792 faces. *Neuropsychologia*, 11(3), 355-362.
- 793 Glezer, L.S., Kim, J., Rule, J., Jiang, X., and Riesenhuber, M. (2015). Adding Words to the Brain’s  
794 Visual Dictionary: Novel Word Learning Selectively Sharpens Orthographic Representations in  
795 the VWFA. *J. Neurosci.*, 35(12), 4965–4972.
- 796 Grill-Spector, K., Knouf, N., and Kanwisher, N. (2004). The fusiform face area subserves face  
797 perception, not generic within-category identification. *Nat. Neurosci.*, 7(5), 555–562.
- 798 Guyader, N., Chauvin, A., Boucart, M., & Peyrin, C. (2017). Do low spatial frequencies explain  
799 the extremely fast saccades towards human faces? *Vis. Res.*, 133, 100-111.
- 800 Haxby, J. V., Ungerleider, L.G., Clark, V.P., Schouten, J.L., Hoffman, E.A., and Martin, A. (1999).  
801 The effect of face inversion on activity in human neural systems for face and object perception.  
802 *Neuron*, 22(1), 189–199.

- 803 Haxby, J., Hoffman, E., Gobbini, M. (2000). The distributed human neural system for face  
804 perception. *Trends Cogn. Sci.*, 4(6), 223–233.
- 805 Heeman, Jessica, Stefan Van der Stigchel, and Jan Theeuwes. The influence of distractors on  
806 express saccades. *J. Vis.*, 17.1 (2017): 35-35.
- 807
- 808 Hellige, J. B. (1996). Hemispheric asymmetry for visual information processing. *Acta*  
809 *Neurobiologiae Experimentalis*, 56, 485-497.
- 810 Honey, C., Kirchner, H., Vanrullen, R. (2008). Faces in the cloud : Fourier power spectrum biases  
811 ultrarapid face detection. *J. Vis.*, 8(12), 1–13.
- 812 Hubel, D. H., & Wiesel, T. N. (1962). Receptive fields, binocular interaction and functional  
813 architecture in the cat's visual cortex. *The Journal of physiology*, 160(1), 106-154.
- 814 Itier, R.J., Taylor, M.J. (2002). Inversion and contrast polarity reversal affect both encoding and  
815 recognition processes of unfamiliar faces: a repetition study using ERPs. *Neuroimage*, 15(2), 353–  
816 372.
- 817 Itier, R.J., Alain, C., Sedore, K., McIntosh, A.R. (2007). Early face processing specificity: it's in  
818 the eyes! *J. Cogn. Neurosci.*, 19(11), 1815–1826.
- 819 Jiang, X., Rosen, E., Zeffiro, T., Vanmeter, J., Blanz, V., Riesenhuber, M. (2006). Evaluation of a  
820 shape-based model of human face discrimination using fMRI and behavioral techniques. *Neuron*,  
821 50(1), 159–172.
- 822 Kanwisher, N., McDermott, J., Chun, M.M. (1997). The Fusiform Face Area : A Module in Human  
823 Extrastriate Cortex Specialized for Face Perception. *J. Neurosci.*, 17(11), 4302–4311.

- 824 Kanwisher, N., Tong, F., Nakayama, K. (1998). The effect of face inversion on the human fusiform  
825 face area. *Cognition*, 68(1), B1–B11.
- 826 Kanwisher, N., & Yovel, G. (2006). The fusiform face area: a cortical region specialized for the  
827 perception of faces. *Philosophical Transactions of the Royal Society of London B: Biological*  
828 *Sciences*, 361(1476), 2109–2128.
- 829 Kirchner, H., and Thorpe, S.J. (2006). Ultra-rapid object detection with saccadic eye movements:  
830 Visual processing speed revisited. *Vis. Res.*, 46(11), 1762–1776.
- 831 Levine, S. C., Banich, M. T., & Koch-Weser, M. P. (1988). Face recognition: A general or specific  
832 rig specific right hemisphere capacity? *Brain and Cognition*, 8(3), 303–325.
- 833 Levy, I., Hasson, U., Avidan, G., Hendler, T., Malach, R. (2001). Center-periphery organization  
834 of human object areas. *Nat. Neurosci.* 4(5), 533–539.
- 835 Liu, J., Harris, A., Kanwisher, N. (2002). Stages of processing in face perception: an MEG study.  
836 *Nat. Neurosci.*, 5(9), 910–916.
- 837 Liu, J., Harris, A., and Kanwisher, N. (2010). Perception of face parts and face configurations: an  
838 fMRI study. *J. Cogn. Neurosci.*, 22(1), 203–211.
- 839 Macknik, S.L., Livingstone, M.S. (1998). Neuronal correlates of visibility and invisibility in the  
840 primate visual system. *Nat. Neuro.*, 1(2), 144–149.
- 841 Macmillan, N. A., & Creelman, C. D. (2005). *Detection Theory: A User's Guide* Lawrence  
842 Erlbaum Associates. New York, 73.
- 843
- 844 Martin, J., Riesenhuber, M., Thorpe, S. (2014). The time-course of face-selective ERP activation  
845 during ultra-rapid saccades. *J. Vis.*, 14(10), 134–134.

- 846 Matsuzaki, N., Schwarzlose, R.F., Nishida, M., Ofen, N., Asano, E. (2015). Upright face-  
847 preferential high-gamma responses in lower-order visual areas: Evidence from intracranial  
848 recordings in children. *Neuroimage*, 109, 249–259.
- 849 Maunsell, J. H., & Newsome, W. T. (1987). Visual processing in monkey extrastriate  
850 cortex. *Annual review of neuroscience*, 10(1), 363-401.
- 851
- 852 Miller, J., Beutinger, D., & Ulrich, R. (2009). Visuospatial attention and redundancy gain. *Psych.*  
853 *Research*, 73(2), 254-262.
- 854
- 855 Mooshagian, E., Kaplan, J., Zaidel, E., & Iacoboni, M. (2008). Fast visuomotor processing of  
856 redundant targets: the role of the right temporo-parietal junction. *PLoS One*, 3(6), e2348.
- 857 Motter, B.C. (2009). Central V4 receptive fields are scaled by the V1 cortical magnification and  
858 correspond to a constant-sized sampling of the V1 surface. *J. Neurosci.*, 29(18), 5749–5757.
- 859 Oostenveld, R., Fries, P., Maris, E., Schoffelen, J.M. (2011). FieldTrip: Open source software for  
860 advanced analysis of MEG, EEG, and invasive electrophysiological data. *Comput. Intell.*  
861 *Neurosci.*, 2011.
- 862 Oosterhof, N.N., Todorov, A. (2008). The functional basis of face evaluation. *Proc. Natl. Acad.*  
863 *Sci.*, 105(32), 11087–11092.
- 864 Perrinet, L. U., Adams, R. A., & Friston, K. J. (2014). Active inference, eye movements and  
865 oculomotor delays. *Biol. Cybernetics*, 108(6), 777-801.
- 866 Pitcher, D., Walsh, V., Yovel, G., Duchaine, B. (2007). TMS evidence for the involvement of the  
867 right occipital face area in early face processing. *Curr. Biol.*, 17(18), 1568–1573.

868 Pizzagalli, D., Regard, M., & Lehmann, D. (1999). Rapid emotional face processing in the  
869 human right and left brain hemispheres: an ERP study. *Neuroreport*, *10*(13), 2691-2698.

870 Poncet, M., Reddy, L., Fabre-thorpe, M. (2012). A need for more information uptake but not  
871 focused attention to access basic-level representations. *J. Vis.*, *12*(1), 1–16.

872 Prieto, E.A., Caharel, S., Henson, R., Rossion, B. (2011). Early (n170/m170) face-sensitivity  
873 despite right lateral occipital brain damage in acquired prosopagnosia. *Front. Hum. Neurosci.*, *5*,  
874 138.

875 Kalesnykas, R.P., Hallett, PE (1987). The differentiation of visually guided and anticipatory  
876 saccades in gap and overlap paradigms. *Exp. Brain Res.*, *68*(1), 115-121.

877 Riesenhuber, M., & Poggio, T. (2002). Neural mechanisms of object recognition. *Current*  
878 *opinion in neurobiology*, *12*(2), 162-168.

879

880 Rhodes, G. (1985). Lateralized processes in face recognition. *British journal of*  
881 *Psychology*, *76*(2), 249-271.

882 Rossion, B., Caharel, S. (2011). ERP evidence for the speed of face categorization in the human  
883 brain: Disentangling the contribution of low-level visual cues from face perception. *Vision Res.*,  
884 *51*(12), 1297–1311.

885 Rousselet, G. A., Husk, J. S., Bennett, P. J., & Sekuler, A. B. (2005). Spatial scaling factors  
886 explain eccentricity effects on face ERPs. *J. Vis.*, *5*(10), 1-1.

887 Rousselet, G.A. (2012). Does filtering preclude us from studying ERP time-courses? *Front.*  
888 *Psychol.*, *3*, 1–9.

- 889 Scholl, C.A., Jiang, X., Martin, J.G., Riesenhuber, M. (2014). Time Course of Shape and Category  
890 Selectivity Revealed by EEG Rapid Adaptation. *J. Cogn. Neurosci.*, 26(2), 408–421.
- 891 Schwarz, W. (1996). Further tests of the interactive race model of divided attention: the effects  
892 of negative bias and varying stimulus—onset asynchronies. *Psychol. Res.*, 58(4), 233-245.
- 893
- 894 Sergent, J., & Bindra, D. (1981). Differential hemispheric processing of faces: Methodological  
895 considerations and reinterpretation. *Psych. Bulletin*, 89(3), 541–554.
- 896 Sherman, S.M. (2016). Thalamus plays a central role in ongoing cortical functioning. *Nat.*  
897 *Neurosci.*, 19(4), 533–541.
- 898 Shigihara, Y., Zeki, S. (2014). Parallel processing of face and house stimuli by V1 and specialized  
899 visual areas: a magnetoencephalographic (MEG) study. *Front. Hum. Neurosci.*, 8, 901.
- 900 Stojanoski, B., Cusack, R. (2014). Time to wave good-bye to phase scrambling: creating controlled  
901 scrambled images using diffeomorphic transformations. *J. Vis.*, 14(12), 1–16.
- 902 Thorpe, S., Fize, D., Marlot, C. (1996). Speed of processing in the human visual system. *Nature*,  
903 381, 520–522.
- 904 Turatto, M., & Betta, E. (2006). Redundant visual signals boost saccade execution. *Psych.*  
905 *Bulletin & Review*, 13(5), 928-932.
- 906 Uyar, F., Shomstein, S., Greenberg, A.S., Behrmann, M. (2015). Retinotopic information interacts  
907 with category selectivity in human ventral cortex. *Neuropsychologia*, 92, 90–106.
- 908 VanRullen, R., Thorpe, S.J. (2001). The time course of visual processing: from early perception  
909 to decision-making. *J. Cogn. Neurosci.*, 13(4), 454–461.

910 Vogels, R., & Orban, G. A. (1996). Coding of stimulus invariances by inferior temporal neurons.

911 In Prog. In *Brain Research*, 112, 195-211.

912 Xu, Y., Liu, J., & Kanwisher, N. (2005). The M170 is selective for faces, not for

913 expertise. *Neuropsychologia*, 43(4), 588-597.

914 Young, A. W., Hay, D. C., & McWeeny, K. H. (1985). Right cerebral hemisphere superiority for

915 constructing facial representations. *Neuropsychologia*, 23(2), 195–202.

916 Yovel, G., Tambini, A., & Brandman, T. (2008). The asymmetry of the fusiform face area is a

917 stable individual characteristic that underlies the left-visual-field superiority for

918 faces. *Neuropsychologia*, 46(13), 3061-3068.

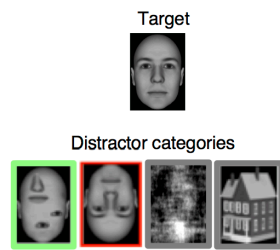
919

920

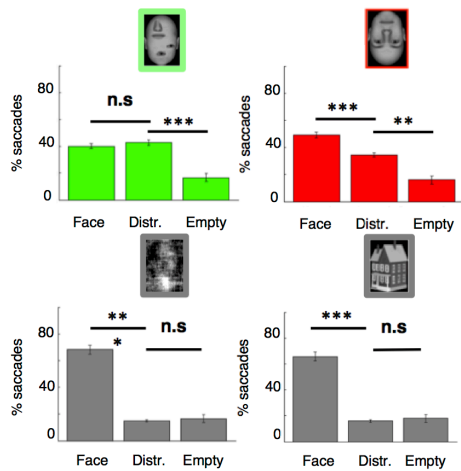
921

A.

Figure 1



B.



C.

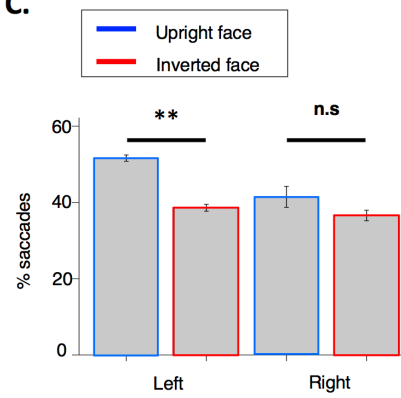


Figure 2

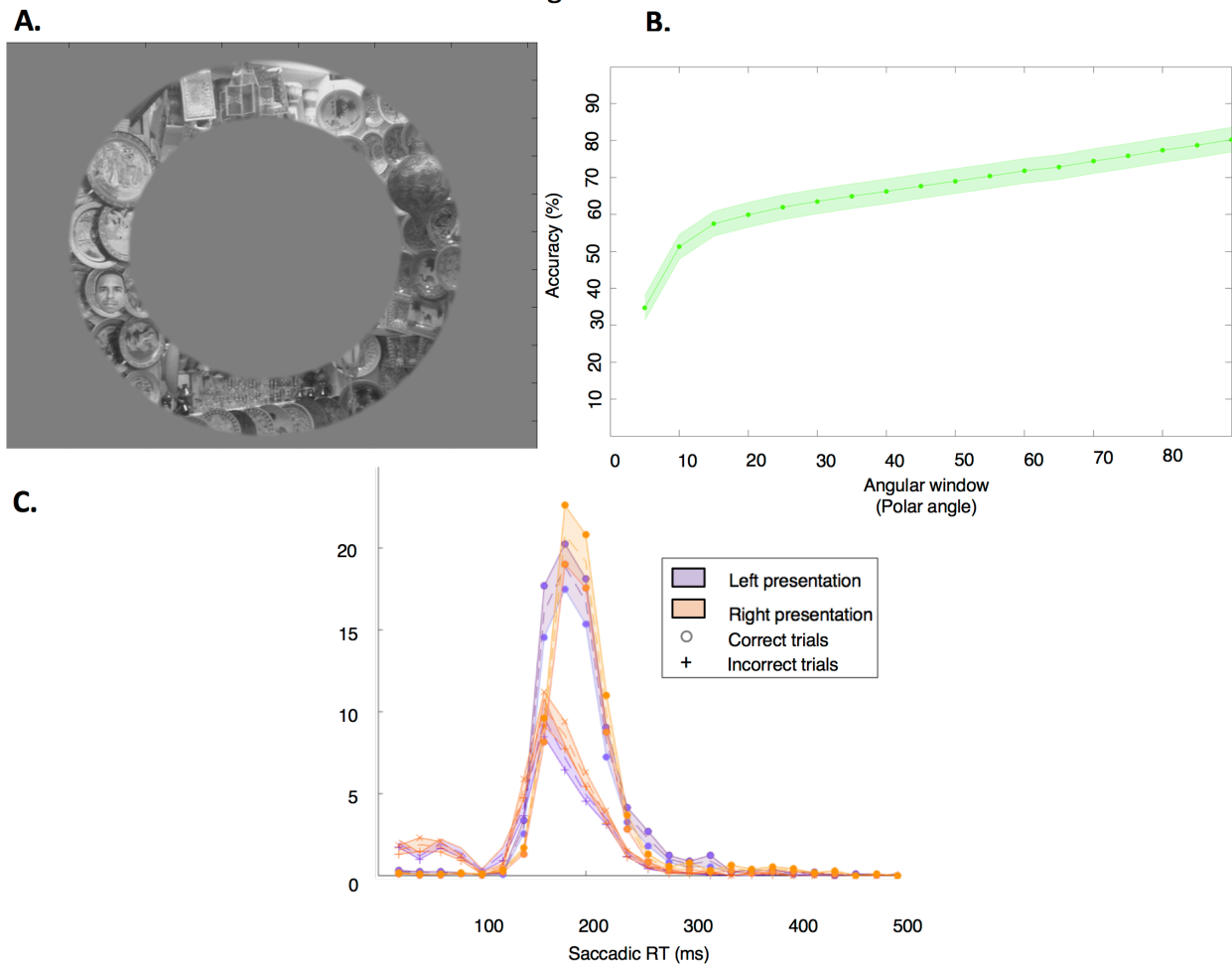


Figure 3

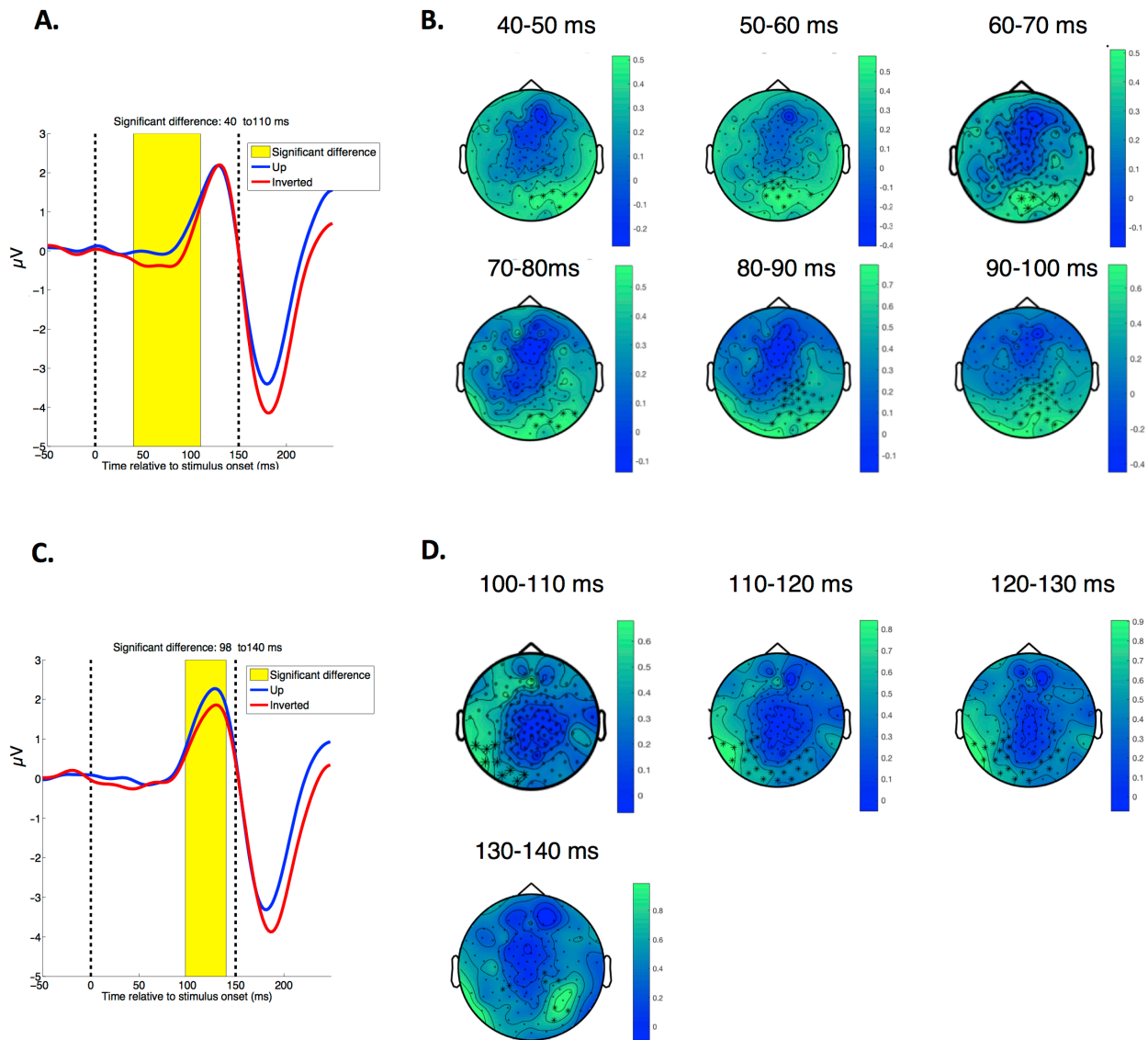
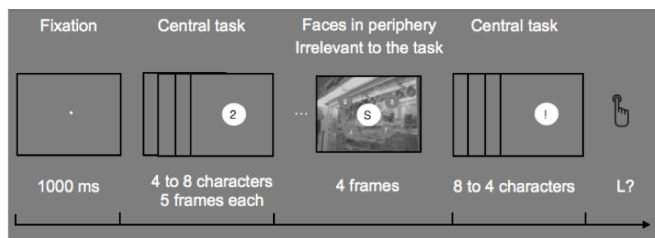


Figure 4

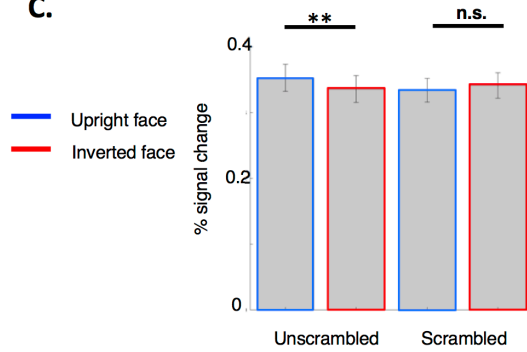
A.



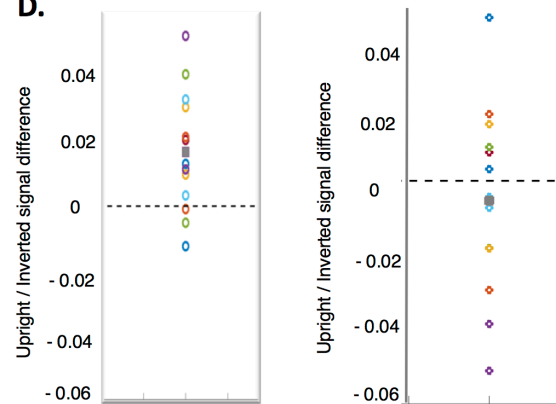
B.



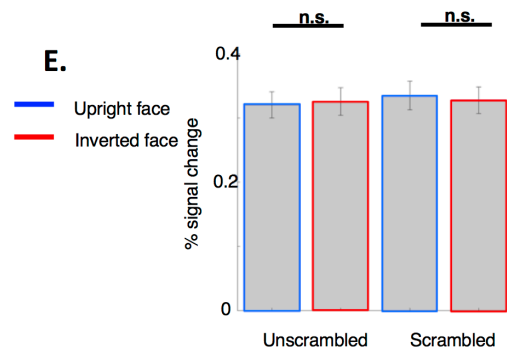
C.



D.



E.



## 922 **Figure Legends**

923 **Figure 1. Experiment 1: Fast saccades toward faces have limited selectivity. A.** Stimuli and  
924 paradigm. At each trial, one face and a distractor (from left to right: a configuration-scrambled  
925 face, an inverted face, a phase-scrambled face, a house) were displayed at 2 positions, here Left  
926 up and Right bottom among 4 positions (Left up, Right up, Left bottom, Right bottom). **B.** Percent  
927 of first saccades landing in the quadrant with the face, with the distractor, or toward one of the  
928 empty quadrants. Results for configuration-scrambled faces are shown in green, for inverted faces  
929 in red, for phase-scrambled faces in gray (left), for houses in gray (right)). In the configuration-  
930 scrambled face condition, saccades were oriented as often toward the configuration-scrambled face  
931 as toward the target (the upright face). When the distractor was an inverted face, saccades were  
932 directed more often toward the target than toward the inverted face distractor. In the control  
933 conditions where distractors were houses and phase-scrambled faces, the percent of saccades  
934 oriented toward the distractor was similar to the percentage of saccades toward an empty quadrant.  
935 **C.** Percent of first saccades in the inverted face condition when the target and the distractor were  
936 either both in the left hemifield, or both in the right hemifield. When they were in the left hemifield,  
937 saccades were more often directed toward the target than toward the distractor. When they were  
938 in the right hemifield, saccades were as often oriented toward the distractor as toward the target.  
939 (\*\*\*)  $p < 0.001$ , \*\*  $p < 0.005$ , \*  $p < 0.05$ ). Data are presented as mean  $\pm$  SEM.

940

941 **Figure 2. Experiment 2: Faces are saccaded to faster when they are in the left hemifield. A.**  
942 Example stimulus. The face target could be pasted anywhere within an annulized natural scene. **B.**  
943 Spatial precision of target saccades in Experiment 2. The plot shows the percentage of saccades

944 landing within an angular window centered on the face, averaged across participants, as a function  
945 of the size of the window (degrees of polar angle). The slope rises steeply up to 15 degrees, as  
946 progressively more face target-directed saccades are included, then becomes shallower with  
947 constant slope, presumably since further increases in window size include progressively more  
948 saccades targeted at distractors. The total size of the window is twice the value indicated in abscissa  
949 since it extends to both sides. This graph thus reveals that most of the saccades aggregated in an  
950 area centered on the face and expanding at  $\pm 15$  degrees of polar angle. **C.** Distribution of saccadic  
951 reaction times for correct and incorrect saccades, for left-presentation and right-presentation of the  
952 faces, averaged across participants. The distribution of correct saccades diverges from the  
953 distribution of incorrect saccades earlier for left than for right presentation. This shows that  
954 saccades start to be selective earlier for left than for right presentations.

955

956 **Figure 3. Experiment 3: EEG data reveal significant face-specific responses starting at 40 ms**  
957 **post-stimulus onset for left-stimulus presentations.** Event-related potentials (ERPs) computed  
958 within the cluster found in the time window [0-150] ms. **Left-presentation group.** **A.** Mean ERPs  
959 elicited by upright versus inverted faces, computed across the channels belonging to the cluster.  
960 The cluster ranges between [40-110] ms post-stimulus. The time window over which the clustering  
961 analysis was run is indicated by dashed lines, the window of significance is in yellow. **B.** Time  
962 course of the cluster, electrodes significant during the whole time window (10 ms bins) are  
963 indicated by stars: the cluster is initially lateralized in the right hemisphere. **Right-presentation**  
964 **group.** **C.** Mean ERPs elicited by upright versus inverted faces, computed across the channels  
965 belonging to the cluster. The cluster ranges between [98-140] ms post-stimulus **D.** Time course  
966 of the cluster, electrodes significant during the whole time window (10 ms bins) are indicated by

967 stars: the cluster is initially lateralized in the left hemisphere. It becomes more spread-out starting  
968 around 110-120 ms poststimulus onset.

969

970 **Figure 4. Experiment 4: fMRI data provide evidence for face-specific responses in V1/V2.**

971 **A.** Example stimuli. Left: example of a face trial, one face is pasted in its 4 different versions  
972 (inverted, upright, scrambled, and inverted scrambled on the top left, top right, bottom left and  
973 bottom right respectively) in the middle of gray circles. Right: example of a house-trial, built in  
974 the same way as the face-trial. **B.** Experimental design. Participants performed a central letter  
975 detection task in a rapid visual serial stream. In this stream, a natural image with faces (or houses)  
976 at 7° eccentricity was displayed at an unpredictable moment. Subjects were not told about the  
977 presence of faces/houses. **C.** Percent signal change within V1/V2 ROIs averaged within stimulus  
978 category across the ROIs activated by left visual presentations (top left and bottom left). There is  
979 a significantly higher percent signal change in trials with upright (unscrambled) faces relatively to  
980 trials with inverted (unscrambled) faces, but no significant difference for the comparison upright  
981 (scrambled) faces versus inverted (scrambled faces). **D.** Left. Representation of the difference  
982 between the percent signal change evoked by the upright (unscrambled) faces and by the inverted  
983 (unscrambled) faces, for left-hemifield presentations. Right. Representation of the difference  
984 between the percent signal change evoked by the upright (scrambled) faces and by the inverted  
985 (scrambled) faces, for left-hemifield presentations. Each dot corresponds to one participant. The  
986 average value of those points is represented by a gray, filled, square. **E.** Percent signal change  
987 averaged within stimulus category across the ROIs activated by right visual presentations (top right  
988 and bottom right). The percent signal change elicited by upright and inverted faces in this visual  
989 hemifield is not significantly different, both for unscrambled and scrambled faces.